**Steel and Composite Structures**, *Vol. 19, No. 5 (2015) 1203-1219*
DOI: http://dx.doi.org/10.12989/scs.2015.19.5.1203 

# Distortional buckling calculation method of steel-concrete composite box beam in negative moment area

Wangbao Zhou*[1], Shujin Li [1a], Lizhong Jiang [2b] and Zhi Huang [2c]

[1] *School of Civil Engineering and Architecture, Wuhan University of Technology, Wuhan, 430070, China*
[2] *School of Civil Engineering, Central South University, Changsha, 410075, China*

(*Received November 10, 2014, Revised April 27, 2015, Accepted April 28, 2015*)

**Abstract.** 'Distortional buckling' is one of the predominant buckling types that may occur in a steel-concrete composite box beam (SCCBB) under a negative moment. The key factors, which affect the buckling modes, are the torsional and lateral restraints of the bottom plate of a SCCBB. Therefore, this article investigates the equivalent lateral and torsional restraint rigidity of the bottom plate of a SCCBB under a negative moment; the results of which show a linear coupling relationship between the applied forces and the lateral and/or torsional restraint stiffness, which are not depended on the cross-sectional properties of a SCCBB completely. The mathematical formulas for calculating the lateral and torsional restraint rigidity of the bottom plate can be used to estimate: (1) the critical distortional buckling stress of SCCBBs under a negative moment; and (2) the critical distortional moment of SCCBBs. This article develops an improved calculation method for SCCBBs on an elastic foundation, which takes into account the coupling effect between the applied forces and the lateral and/or torsional restraint rigidity of the bottom plate. This article analyzes the accuracy of the following calculation methods by using 24 examples of SCCBBs: (1) the conventional energy method; (2) the improved calculation method, as it has been derived in this article; and (3) the ANSYS finite element method. The results verify that the improved calculation method, as it has been proved in this article, is more accurate and reliable than that of the current energy method, which has been noted in the references.

**Keywords:** steel-concrete composite box beam; elastic foundation beam method; distortional buckling; rotational restraint stiffness; lateral restraint stiffness

## 1. Introduction

The steel-concrete composite box beam (SCCBB) is an important type of lateral-load-carrying composite element, in which shear connections attach the concrete slab to a steel-box beam, and, thereby allow the steel-box beam and concrete slab to carry loads jointly (Ipe *et al*. 2013, Li *et al*. 2014). The salient characteristics of a SCCBB are as following: they are light-weight, they have

*Corresponding author, Ph.D., E-mail: zhwb@whut.edu.cn
[a] Ph.D., E-mail: whutlsj@163.com
[b] Ph.D., E-mail: lzhjiang@csu.edu.cn
[c] Ph.D., E-mail: zzh10@psu.edu


http://www.techno-press.org/?journal=scs&subpage=8 ISSN: 1229-9367 (Print), 1598-6233 (Online)

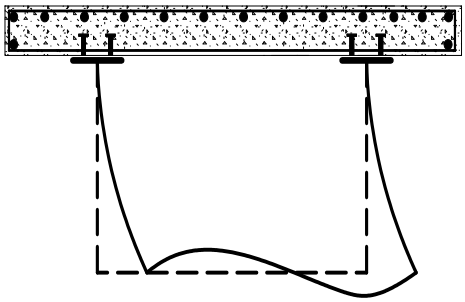

Fig. 1 Distortional buckling of a SCCBB under a negative moment

strong torsional resistance, and they are very good in durability. These types of components possess a high compressive resistance owing to concrete and an excellent tensile resistance owing to steel-box beam. Besides, SCCBB is an environment-friendly structure (Zhou *et al*. 2015). Being an economical and reasonable structure, SCCBBs are widely being used throughout the world for composite girders and slab systems (Gara *et al*. 2011, Champenoy *et al*. 2014). Distortional buckling is an important type of buckling specific to SCCBBs, which differs from the conventional lateral-torsional buckling and usually occurs in the hogging regions of SCCBBs. Fig. 1 shows that the distortional buckling of a SCCBB may cause simultaneous web deformation and lateral-torsional deflection of the bottom plate owing to the restraint of the concrete slab (Chen 2005, Jia and Chen 2009, Chen and Jia 2010).The findings relating to the ultimate bearing capacity of a continuous I-steel concrete composite beam disclosed that the distortional buckling, the local buckling, or alternatively an interactive mode of both previously mentioned buckling govern the ultimate bearing capacity (Chen 1992, 2005, Jia and Chen 2009, Chen and Jia 2010). In fact, the above findings were earlier reported by the Swedish code for light-gauge metal structures in 1982, when they deemed the distortional buckling analysis of an I-steel-concrete composite beam in a negative moment area to be an elastic foundation beam under constant axial force, i.e., the method of elastic foundation beam under constant axial force (Swedish Institute of Steel Construction 1982). British Bridge Standard [BS5400] (British Standards Institution 1982) also employs the aforementioned method for the design of steel-concrete continuous composite beams. Svensson (1985), Williams and Jemah (1987), and Goltermann and Svensson (1988) have suggested to increase the area involved in the steel-beam web, thereby improved the elastic foundation beam method; they use the restraint stiffness as a constant cross-sectional property and do not consider the coupling effect between the applied forces and the lateral and/or torsional restraint stiffness of the steel-beam bottom plate. The British Steel Structure Institute (Lawson and Rackham 1989) used another energy method often employed to compute the distortional buckling of I-steel-concrete composite beams, which gives a way to determine the critical buckling stress of an I-steel-concrete composite beam under a negative moment. Owing to the limited capacity of computation at that era, the aforementioned studies had not carried out the detailed analyses for the application of elastic foundation beam method in distortional buckling analysis of the steel-concrete composite beams. Chen and Ye (2010) and Ye and Chen (2013) suggested revising the involved part of the web of the I-steel-concrete composite beam, which is based on Svensson's elastic foundation beam model, in which they discovered that the elastic foundation beam method was more reasonable than that of the energy method for distortional buckling of the I-steel-concrete composite beam. On the basis of their research, Zhou *et al*. (2012) proposed a way

to indicate the linear coupling relationship between the applied forces and the torsional and/or lateral restraint stiffness of the bottom flange.

The aforementioned studies mostly concentrate on the study of I-steel-concrete composite beam, whereas the research on the usefulness of a SCCBB does exist but of limited scope. Jiang *et al*. (2013) presented a calculation model of SCCBB on the basis of stability analysis. By using energy method, they determined the formulas to calculate the critical bending moment of distortional and local buckling. Next, the researchers had not reported the distortional buckling of a SCCBB by using the elastic foundation beam method.

On the basis of the coupling effect between the applied forces and restraint stiffness of the bottom plate, this article determines a way to calculate the lateral and torsional restraint stiffness of the bottom plate of a SCCBB under a negative uniform moment, thereby suggesting improvements in the elastic foundation beam method. This article further develops a way to calculate the critical distortional moment of a SCCBB by taking into account the coupling effect between the applied forces and the lateral and/or torsional restraint stiffness. To conclude, this article analyzes the accuracy of both the proposed mathematical models and the existing energy calculation methods by the way of examination of 24 examples. The proposed method provides a theoretical basis of further research for the analysis of distortional buckling considering the moment gradient and the ultimate bearing capacity of a SCCBB.

## 2. Restraining stiffness analysis of a SCCBB's web

Fig. 2 depicts the cross-sectional dimensions of a SCCBB and its coordinate system. The distortional buckling of a SCCBB occurs along with the lateral deformation of the steel web, as it has been shown in Fig. 1. To simplify the calculations, the following assumptions have been formulated (Johnson and Fan 1991, Bradford and Gao 1992, Bradford and Kemp 2000, Tong and Xia 2007, Jia and Chen 2009, Chen and Jia 2010): (1) the lateral and torsional stiffness of the concrete slab are relatively higher, therefore, the top flange of the steel-box beam is restricted by the concrete slab; (2) the tensile resistance of the concrete slab is ignored; and (3) the vertical pre-buckling deformation of a SCCBB is neglected.

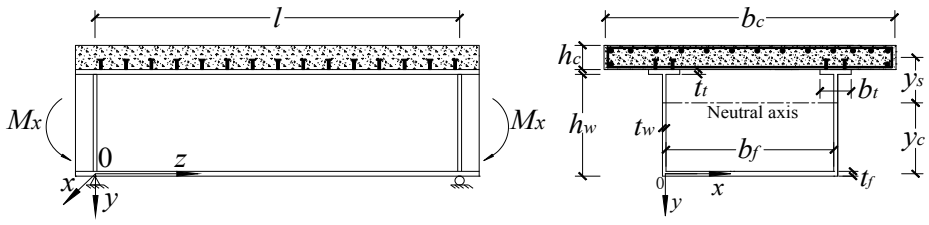


Fig. 2 Cross-sectional dimensions of a SCCBB and its coordinate system

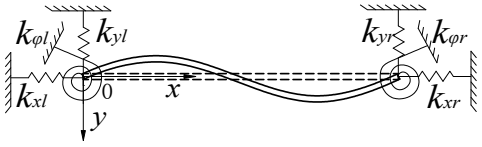


Fig. 3 Simplified calculation model of a SCCBB

In accordance with the above assumptions, the buckling model of a SCCBB can be simplified as it has been shown in the model (refer to Fig. 3), where the horizontal, torsional and vertical directions of both longitudinal edges of the bottom plate are restricted by springs. The vertical bend deformation, which occurred before the buckling of a SCCBB, is a stable deformation and does not occur again during the buckling of a SCCBB. Therefore, the springs of both longitudinal edges of the bottom plate in the vertical direction can be seen as rigid restraints (i.e., $k_{yl} = k_{yr} = \infty$).

By considering the longitudinal reinforcements within the concrete slab of a SCCBB in a negative moment area, the compressive stress exerted on the bottom edge of the web can be expressed as (Bradford 1988)

$$\sigma_1(z) = M_x y_c / I \tag{1}$$

$$y_c = \frac{A_s y_s + A_t h_w + 0.5 A_w h_w}{A_s + A_t + A_w + A_f} \tag{2}$$

$$A_t = 2 b_t t_t, \quad A_w = 2 h_w t_w, \quad A_f = b_f t_f \tag{3}$$

where, $A_s$ denotes the cross-sectional area of the longitudinal reinforcements within the concrete slab, as it has been shown in Fig. 1, $y_c$ denotes the distance between the neutral axis and the bottom plate, $y_s$ denotes the distance between the neutral axis and the center of gravity of the longitudinal reinforcements within the concrete slab, $h_w$ and $t_w$ denote the height and thickness of the web of a steel beam respectively, $b_f$ and $t_f$ denote the width and thickness of the bottom plate of the steel beam respectively, $b_t$ and $t_t$ denote the width and thickness of the top flange of the steel beam respectively. $M_x$ denotes the negative uniform moment acting on a SCCBB, $I$ denotes the moment of inertia of the equivalent cross-section of a SCCBB.

### *2.1 Rotation restraint stiffness analysis for the web of a SCCBB*

Fig. 4 shows the simplified model of the steel-box beam web, in which two transversal edges are simply supported at the ends. The junction between the web and the top flange remains fixed, whereas the junction between the web and the bottom plate is simply supported (Bradford and Kemp 2000, Chen 2005, Jia and Chen 2009, Chen and Jia 2010). The boundary conditions of the steel-box beam web can mathematically be expressed as follows (Chen 2005, Jia and Chen 2009, Chen and Jia 2010, Zhou and Jiang 2014)

$$\begin{cases} \left.\dfrac{\partial w}{\partial y}\right|_{y=-h_w} = 0 \qquad w\big|_{z=0,\lambda} = 0 \qquad w\big|_{y=0,-h_w} = 0 \\ \left. D_w\left(\dfrac{\partial^2 w}{\partial z^2} + \mu \dfrac{\partial^2 w}{\partial y^2}\right)\right|_{z=0,\lambda} = 0 \end{cases} \tag{4}$$

where, $D_w = E t_w^3 / 12(1-\mu^2)$, $\mu$ denotes the Poisson's ratio of steel, $E$ denotes the elasticity modulus of steel beam, $w$ denotes the buckling deformation function of a steel-box beam web, $\lambda = l/n$, $n$ denotes the number of half wave, and $l$ denotes the length of a SCCBB.

The lateral deformation of the left web of a SCCBB can mathematically be expressed as a combination of cubic polynomial function $f_1(y)$ and trigonometric function that can be written as

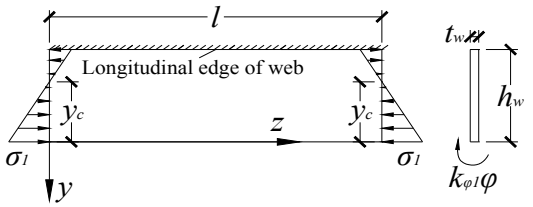


Fig. 4 Web of a SCCBB under a compressive stress and a distributed moment

(Jiang *et al*. 2013)

$$w_l = f_1(y)\left(c_l \sin\frac{\pi z}{\lambda}\right) \tag{5}$$

In accordance with the boundary conditions, the cubic polynomial function $f_1(y)$ can be expressed as follows

$$f_1(y) = \frac{y}{h_w} + 2\left(\frac{y}{h_w}\right)^2 + \left(\frac{y}{h_w}\right)^3 \tag{6}$$

Next, the buckling deformation function of the left web of the SCCBB can be expressed as follows

$$w_l = c_l\left[\frac{y}{h_w} + 2\left(\frac{y}{h_w}\right)^2 + \left(\frac{y}{h_w}\right)^3\right]\sin\frac{\pi z}{\lambda} \tag{7}$$

The rotational angle of the left longitudinal edge of the bottom plate can be expressed as follows

$$\varphi_l = \left.\frac{\partial w_l}{\partial y}\right|_{y=0} = \frac{c_l}{h_w}\sin\frac{\pi z}{\lambda} \tag{8}$$

The bending strain energy of the left web of a SCCBB can be obtained in accordance with the tiny deflection theory (Jiang and Qi 2013), which can be written as

$$U_1 = \frac{D_w}{2}\int_0^{\lambda}\int_{-h_w}^{0}\left[\left(\frac{\partial^2 w_l}{\partial y^2}\right)^2 + \left(\frac{\partial^2 w_l}{\partial z^2}\right)^2 + 2\mu\frac{\partial^2 w_l}{\partial y^2}\frac{\partial^2 w_l}{\partial z^2} + 2(1-\mu)\left(\frac{\partial^2 w_l}{\partial z \partial z}\right)^2\right]\mathrm{dydz} \tag{9}$$

Substituting Eq. (7) into Eq. (9) leads to the bending strain energy of the left web of a SCCBB as follows

$$U_1 = \frac{\lambda D_w c_l^2}{2}\left[\frac{2}{h_w^3} + \frac{2}{15h_w}\beta + \frac{h_w}{210}\beta^2\right] \tag{10}$$

The deformation energy of the spring restraint of the left web can be written as

$$U_2 = \frac{k_{\varphi 1}}{2}\int_0^{\lambda}\left(\left.\frac{\partial w_l}{\partial y}\right|_{y=0}\right)^2 \mathrm{dz} \tag{11}$$

Substituting Eq. (7) into Eq. (11) leads to deformation energy of the spring restraint of the left web as follows

$$U_2 = \frac{\lambda k_{\varphi_{l1}} c_l^2}{4h_w^2} \tag{12}$$

The external work of the left web of a SCCBB is equal to

$$W = t_w \int_0^{\lambda} \int_{-h_w}^{0} \left[ \frac{\sigma_1 (y_c + y)}{2y_c} \left( \frac{\partial w_l}{\partial z} \right)^2 \right] \mathrm{dydz} \tag{13}$$

Substituting Eq. (7) into Eq. (13) leads to the external work of the left web of a SCCBB as follows

$$W = \left( \frac{1}{420} - \frac{h_w}{1120 y_c} \right) \lambda \beta \sigma_1 t_w h_w c_l^2 \tag{14}$$

The total potential energy of the distortional buckling of a SCCBB can mathematically be expressed as

$$\Pi = U_1 + U_2 - W \tag{15}$$

According to the principle of minimum total potential energy, the following relations can be formulated (Liu *et al*. 2014, Ruocco and Minutolo 2014)

$$\left( B_0 + k_{\varphi_{l1}} T - \sigma_1 N_0 \right) c_l = 0 \tag{16}$$

where

$$B_0 = \lambda D_w \left( \frac{2}{h_w^3} + \frac{h_w \beta^2}{210} + \frac{2\beta}{15 h_w} \right) \tag{17}$$

$$N_0 = \lambda \beta \left( \frac{t_w h_w}{210} - \frac{t_w h_w^2}{560 y_c} \right) \tag{18}$$

$$T = \frac{\lambda}{2h_w^2} \tag{19}$$

where, $\beta = \pi^2 / \lambda^2$, $k_{\varphi_{l1}}$ denotes the rotational restraint stiffness of the left web, and $c_l$ denotes the general coordinates representing the distortional buckling deformation of the left web.

The general coordinates $c_l$ cannot be equal to zero, subject to the distortional buckling of a SCCBB when it occurs. Therefore, the rotational restraint stiffness $k_{\varphi_{l1}}$ can be solved with the eigenvalue of the following characteristic matrix

$$\left| B_0 + k_{\varphi_{l1}} T - \sigma_1 N_0 \right| = 0 \tag{20}$$

$$k_{\varphi_{l1}} = \frac{\sigma_1 N_0 - B_0}{T} \tag{21}$$

Eq. (21) shows a linear coupling relationship, which exists between the applied forces and the rotational restraint stiffness of the left web of a SCCBB. This detection indicates that the rotational restraint stiffness of the left web may not only be determined by using the features of a SCCBB's cross-section, but it can also be depended on the applied forces. As a consequence, it may not be appropriate to use the restraint stiffness as a constant, which relates to the cross-sectional features of a SCCBB.

According to the theory of elastic thin plate, the lateral distribution force exerted on the bottom edge of the left web can be expressed as follows (Timoshenko 2009, Atanackovic and Guran 2012)

$$f_{x\varphi_l} = -D_w\left[\frac{\partial^3 w_l}{\partial y^3} + (2-\mu)\frac{\partial^3 w_l}{\partial z^2 \partial y}\right] \tag{22}$$

$$f_{x\varphi_l}\Big|_{y=0} = \left[\frac{(2-\mu)\beta}{h_w} - \frac{6}{h_w^3}\right] D_w c_l \sin\frac{\pi z}{\lambda} \tag{23}$$

The lateral deformation of the right web of a SCCBB can be expressed by virtue of a combination of cubic polynomial function $f_2(y)$ and trigonometric function in the following manner (Jiang *et al*. 2013)

$$w_r = f_2(y)\left(c_r \sin\frac{\pi z}{\lambda}\right) \tag{24}$$

In the same way as of the left web and according to the principle of minimum total potential energy, the following equations relating to the right web of a SCCBB can be written

$$w_r = c_r\left[\frac{y}{h_w} + 2\left(\frac{y}{h_w}\right)^2 + \left(\frac{y}{h_w}\right)^3\right]\sin\frac{\pi z}{\lambda} \tag{25}$$

$$\left(B_0 + k_{\varphi_{r1}} T - \sigma_1 N_0\right) c_r = 0 \tag{26}$$

$$f_{x\varphi_r}\Big|_{y=0} = D_w\left[\frac{(2-\mu)\beta}{h_w} - \frac{6}{h_w^3}\right] c_r \sin\frac{\pi z}{\lambda} \tag{27}$$

where, $k_{\varphi_{r1}}$ denotes the rotational restraint stiffness of the right web, $f_{x\varphi_r}$ denotes the lateral distribution force exerted on the bottom edge of the right web, and $c_r$ denotes the general coordinates representing the distortional buckling deformation of the right web.

The rotational angle of the right longitudinal edge of the bottom plate can be expressed as follows

$$\varphi_r = \frac{\partial w_r}{\partial y}\bigg|_{y=0} = \frac{c_r}{h_w}\sin\frac{\pi z}{\lambda} \tag{28}$$

The general coordinates $c_r$ cannot be equal to zero, when the distortional buckling of a SCCBB occurs. Therefore, the rotational restraint stiffness $k_{\varphi_{r1}}$ can be solved with the eigenvalue of the following characteristic matrix

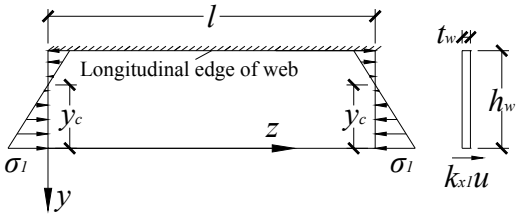


Fig. 5 Web of a SCCBB under compressive stress and lateral distributed stress

$$\left|B_0 + k_{\varphi_{r1}} T - \sigma_1 N_0\right| = 0 \tag{29}$$

When solving Eq. (29), the rotational restraint stiffness can be obtained, which is given by

$$k_{\varphi_{r1}} = \frac{\sigma_1 N_0 - B_0}{T} \tag{30}$$

Eq. (30) shows that a linear coupling relationship exists between the applied forces and the rotational restraint stiffness of the right web.

### *2.2 Lateral restraint stiffness analysis for the web of a SCCBB*

Fig. 5 illustrates a simplified model of the web of a SCCBB. The two transversal edges are supported simply, and the web and the top flange have a fixed junction (Jia and Chen 2009, Chen and Jia 2010). In the longitudinal direction, the junction between the web and the bottom plate is free. The boundary conditions of the web can mathematically be expressed as follows

$$\begin{cases} \left.\dfrac{\partial w}{\partial y}\right|_{y=0,-h_w} = 0 \qquad w\big|_{z=0,\lambda} = 0 \qquad w\big|_{y=-h_w} = 0 \\ \left. D_w\left(\dfrac{\partial^2 w}{\partial z^2} + \mu\dfrac{\partial^2 w}{\partial y^2}\right)\right|_{z=0,\lambda} = 0 \end{cases} \tag{31}$$

The lateral deformation of either the left or right web of a SCCBB can mathematically be expressed by using a combination of cubic polynomial function $f_3(y)$ and trigonometric function in the following manner (Jiang and Qi 2013)

$$w = f_3(y)\left(d\sin\frac{\pi z}{\lambda}\right) \tag{32}$$

According to the Eq. (31), the cubic polynomial function $f_3(y)$ can be expressed as follows

$$f_3(y) = 1 - 3\left(\frac{y}{h_w}\right)^2 - 2\left(\frac{y}{h_w}\right)^3 \tag{33}$$

Therefore, the distortional buckling deformation function of both the left and right web of a SCCBB can be expressed as follows

$$w = d\left[1-3\left(\frac{y}{h_w}\right)^2-2\left(\frac{y}{h_w}\right)^3\right]\sin\frac{\pi z}{\lambda} \tag{34}$$

The lateral displacement function of the bottom plate can be expressed as follows

$$u = w\big|_{y=0} = d\sin\frac{\pi z}{\lambda} \tag{35}$$

Similarly, in accordance with the principle of minimum total potential energy (Ruocco and Minutolo 2014), the following relations can be formulated

$$\left(H_0 + k_{x1}R - \sigma_1 S_0\right)d = 0 \tag{36}$$

where

$$S_0 = \lambda\beta t_w\left(\frac{13h_w}{70}-\frac{3h_w^2}{70y_c}\right) \tag{37}$$

$$H_0 = \lambda D_w\left(\frac{6}{h_w^3}+\frac{13\beta^2 h_w}{70}+\frac{6\beta}{5h_w}\right) \tag{38}$$

$$R = \frac{\lambda}{2} \tag{39}$$

where, $k_{x1}$ denotes the lateral restraint stiffness of either the left or right web, and $d$ denotes the general coordinates representing the distortional buckling deformation of the web.

The general coordinates $d$ cannot be equal to zero, when distortional buckling occurs, and, therefore, the lateral restraint stiffness $k_{x1}$ of either the left or right web can be solved by the eigenvalue of the following characteristic matrix

$$\left|H_0 + k_{x1}R - \sigma_1 S_0\right| = 0 \tag{40}$$

When solving Eq. (40), the lateral restraint stiffness of either the left or right web can be obtained, which is written as

$$k_{x1} = \frac{\sigma_1 S_0 - H_0}{R} \tag{41}$$

Eq. (41) determines that a relationship based on linear coupling exists between the applied forces and the lateral restraint stiffness of either the left or right web.

According to the theory of elastic thin plate, the lateral distribution force of either the left or right web can mathematically be expressed as follows (Timoshenko 2009, Atanackovic and Guran A 2012)

$$f_{\varphi x} = -D_w\left(\frac{\partial^2 w}{\partial y^2}+\mu\frac{\partial^2 w}{\partial z^2}\right) \tag{42}$$

$$f_{\varphi x}\big|_{y=0} = \left(6/h_w^2+\mu\beta\right)D_w d\sin\frac{\pi z}{\lambda} \tag{43}$$

## 3. Distortional buckling method of a SCCBB

As it has been shown in Fig. 3, where the function of out-of-plane deformation of the bottom plate is $v(x, z)$, therefore, the boundary condition of the bottom plate can be written as

$$\begin{cases} v\big|_{x=0} = 0 \quad v_{,x}\big|_{x=0} = \varphi_l(z) \\ v\big|_{x=b_f} = 0 \quad v_{,x}\big|_{x=b_f} = \varphi_r(z) \end{cases} \tag{44}$$

The function of out-of-plane buckling deformation of the bottom plate can be expressed by using the trigonometric functions in the following manner (Jiang and Qi 2013)

$$v = f_4(x)\varphi_l(z) + f_5(x)\varphi_r(z) \tag{45}$$

According the boundary conditions, the trigonometric functions $f_4(y)$ and $f_5(y)$ can be given as

$$f_4(x) = \frac{b_f}{2\pi}\sin\frac{\pi x}{b_f} + \frac{b_f}{4\pi}\sin\frac{2\pi x}{b_f} \tag{46}$$

$$f_5(x) = \frac{b_f}{4\pi}\sin\frac{2\pi x}{b_f} - \frac{b_f}{2\pi}\sin\frac{\pi x}{b_f} \tag{47}$$

Therefore, the function of out-of-plane buckling deformation of the bottom plate can be written as

$$v = \frac{b_f}{2\pi}(\varphi_l - \varphi_r)\sin\frac{\pi x}{b_f} + \frac{b_f}{4\pi}(\varphi_l + \varphi_r)\sin\frac{2\pi x}{b_f} \tag{48}$$

Similarly, according to the principle of minimum total potential energy, the neutral equilibrium differential equation of the bottom plate can be written as

$$\begin{cases} D_f\left(\frac{5\pi^2\varphi_l}{8b_f} + \frac{3\pi^2\varphi_r}{8b_f} - \frac{b_f\varphi_l''}{2} + \frac{5b_f^3\varphi_l''''}{32\pi^2} - \frac{3b_f^3\varphi_r''''}{32\pi^2}\right) + \left(\frac{5\sigma_1 A_f b_f^2\varphi_l'}{32\pi^2}\right)' - \left(\frac{3\sigma_1 A_f b_f^2\varphi_r'}{32\pi^2}\right)' + k_{\varphi_l}\varphi_l + f_{\varphi x} = 0 \\ 2k_x u + \left(\sigma_1 A_f u'\right)' + EI_y u'''' - f_{x\varphi_l} - f_{x\varphi_r} = 0 \\ D_f\left(\frac{5\pi^2\varphi_r}{8b_f} + \frac{3\pi^2\varphi_l}{8b_f} - \frac{b_f\varphi_r''}{2} + \frac{5b_f^3\varphi_r''''}{32\pi^2} - \frac{3b_f^3\varphi_l''''}{32\pi^2}\right) + \left(\frac{5\sigma_1 A_f b_f^2\varphi_r'}{32\pi^2}\right)' - \left(\frac{3\sigma_1 A_f b_f^2\varphi_l'}{32\pi^2}\right)' + k_{\varphi_r}\varphi_r + f_{\varphi x} = 0 \end{cases} \tag{49}$$

$$k_{\varphi_l} = k_{\varphi_r} = -k_{\varphi_r 1} = \frac{B_0 - \sigma_1 N_0}{T}, \quad k_x = -k_{x1} = \frac{H_0 - \sigma_1 S_0}{R} \tag{50}$$

where, $I_y = t_f b_f^3/12$, $D_f = Et_f^3/12(1-\mu^2)$, $k_{\varphi_l}$ and $k_{\varphi_r}$ denote the torsional restraint stiffness of the left and right edges of the bottom plate respectively, and $k_x$ denotes the lateral restraint stiffness of the bottom plate.

By employing the Galerkin method (Jaberzadeh *et al*. 2013, Tinh and Minh 2013, Wang and Peng 2013) in the solution of Eq. (49), the following relations can be derived

$$\begin{cases} \int_0^{\lambda}\left[ D_f\left( \frac{5\pi^2\varphi_l}{8b_f}+\frac{3\pi^2\varphi_r}{8b_f}-\frac{b_f\varphi_l''}{2}+\frac{5b_f^3\varphi_l''''}{32\pi^2}-\frac{3b_f^3\varphi_r''''}{32\pi^2}\right)+\left(\frac{5\sigma_1 A_f b_f^2\varphi_l'}{32\pi^2}\right)'-\left(\frac{3\sigma_1 A_f b_f^2\varphi_r'}{32\pi^2}\right)'+k_{\varphi_l}\varphi_l+f_{\varphi x}\right]\sin\frac{\pi z}{\lambda}dz=0 \\ \int_0^{\lambda}\left[2k_x u+\left(\sigma_1 A_f u'\right)'+EI_y u''''-f_{x\varphi_l}-f_{x\varphi_r}\right]\sin\frac{\pi z}{\lambda}dz=0 \\ \int_0^{\lambda}\left[ D_f\left( \frac{5\pi^2\varphi_r}{8b_f}+\frac{3\pi^2\varphi_l}{8b_f}-\frac{b_f\varphi_r''}{2}+\frac{5b_f^3\varphi_r''''}{32\pi^2}-\frac{3b_f^3\varphi_l''''}{32\pi^2}\right)+\left(\frac{5\sigma_1 A_f b_f^2\varphi_r'}{32\pi^2}\right)'-\left(\frac{3\sigma_1 A_f b_f^2\varphi_l'}{32\pi^2}\right)'+k_{\varphi_r}\varphi_r+f_{\varphi x}\right]\sin\frac{\pi z}{\lambda}dz=0 \end{cases} \tag{51}$$

$$\begin{pmatrix} B_1+k_{\varphi_l}T-\sigma_1 N_1 & F+0.6\sigma_1 N_1 & Q \\ F+0.6\sigma_1 N_1 & B_1+k_{\varphi_r}T-\sigma_1 N_1 & Q \\ P & P & H_1-\sigma_1 S_1+2k_x R \end{pmatrix}\boldsymbol{\eta}=0 \tag{52}$$

where

$$B_1=\frac{5D_f\pi^2\lambda}{16b_f h_w^2}+\frac{D_f b_f\beta\lambda}{4h_w^2}+\frac{5D_f b_f^3\beta}{64\lambda h_w^2} \tag{53}$$

$$H_1=0.5EI_y\beta^2\lambda \qquad S_1=0.5A_f\lambda\beta \tag{54}$$

$$N_1=\frac{5A_f b_f^2}{64h_w^2\lambda} \quad Q=\frac{3D_w\lambda}{h_w^3}+\frac{\lambda D_w\mu\beta}{2h_w} \tag{55}$$

$$P=\frac{3D_w\lambda}{h_w^3}-\frac{D_w(2-\mu)\lambda\beta}{2h_w} \tag{56}$$

$$F=\frac{3D_f\pi^2\lambda}{16b_f h_w^2}-\frac{3D_f b_f^3\beta}{64\lambda h_w^2} \tag{57}$$

$$\boldsymbol{\eta}=(c_l,c_r,d)^T \tag{58}$$

Since the functions of theoretical distortional buckling deformation, as they have introduced in this article, cannot accurately describe the buckling deformation of the actual models, and this can only be realized by increasing the additional constraints to the actual model. Therefore, (1) the restraint stiffness as it has been introduced in this article is higher than that of the real model, and (2) the critical distortional buckling stress as it has been calculated by theoretical method is greater than that of the actual model. To eliminate errors, this article recommends a reduction factor to be applied to the torsional restraint stiffness of the bottom plate; the value of which is found to be 0.5.

The combination of Eqs. (50) and (52) leads to

$$\left[\begin{pmatrix} B & F & Q \\ F & B & Q \\ P & P & H \end{pmatrix}-\sigma_1\begin{pmatrix} N & -0.6N_1 & 0 \\ -0.6N_1 & N & 0 \\ 0 & 0 & S \end{pmatrix}\right]\boldsymbol{\eta}=0 \tag{59}$$

where

$$\begin{cases} B = B_0/2 + B_1 & N = N_0/2 + N_1 \\ H = 2H_0 + H_1 & S = 2S_0 + S_1 \end{cases} \tag{60}$$

The deformation vector $\eta$ cannot be equal to 0, when distortional buckling of a SCCBB occurs. Therefore, the distortional buckling of a SCCBB can be solved by the eigenvalue of the following characteristic matrix

$$\left| \begin{pmatrix} B & F & Q \\ F & B & Q \\ P & P & H \end{pmatrix} - \sigma_1 \begin{pmatrix} N & -0.6N_1 & 0 \\ -0.6N_1 & N & 0 \\ 0 & 0 & S \end{pmatrix} \right| = 0 \tag{61}$$

When solving Eq. (61), the critical buckling stress of a SCCBB can be obtained, which is given by

$$\sigma_{cr} = \min\{\sigma_{t1}, \sigma_{t2}\} \tag{62}$$

where

$$\sigma_{t1} = \frac{B - F}{N + 0.6N_1} \tag{63}$$

$$\sigma_{t2} = \frac{-\gamma_2 - \sqrt{\gamma_2^2 - 4\gamma_1\gamma_3}}{2\gamma_1} \tag{64}$$

$$\sigma_{t3} = \frac{-\gamma_2 + \sqrt{\gamma_2^2 - 4\gamma_1\gamma_3}}{2\gamma_1} \tag{65}$$

$$\gamma_1 = NS - 0.6N_1S \tag{66}$$

$$\gamma_2 = 0.6N_1H - NH - BS - FS \tag{67}$$

$$\gamma_3 = BH + FH - 2PQ \tag{68}$$

$\sigma_{cr}$ denotes the critical buckling stress of a SCCBB and the following equation can be used to calculate the critical distortional buckling moment of a SCCBB

$$M_{cr} = \sigma_{cr} I / y_c \tag{69}$$

## 4. Analysis of examples

Both, the calculation method as it has been introduced in this article and the finite element method, were employed to analyze the distortional buckling of 24 examples of a SCCBB under a negative uniform moment. To validate the calculation method, as it has been proposed in this paper, Jiang's method (Jiang *et al*. 2013) based on energy method was employed to calculate the distortional buckling in the aforementioned 24 examples. This article uses *ANSYS* commercial

software to conduct finite element analysis. The steel beam was modeled using a 4-node, quadrilateral, shell 181 elements. The aspect ratio of the mesh is kept close to 1, the mean mesh size varies between 0.1 m and 0.15 m, and approximately 48,000 finite elements were employed in the model. The Young's modulus is equal to $2.06 \times 10^5$ N/mm$^2$, whereas the Poisson's ratio is 0.3 and the yield strength is 345 MPa. The numerical simulations have been performed to represent the concrete slab of a SCCBB as constraints (Ye and Chen 2013). The end moments were exerted directly at the end of the model in the form of a stress gradient. The two degrees of freedom at two ends of beams in x- and y- directions are restrained and the torsion at the ends of a beam is thus restrained. The degree of freedom of one node at the left end in z-direction is restrained to meet the static balance requirements. In addition, two degrees of freedom of the top flange in x-and y-directions are restricted in the eigenvalue buckling analysis. Tables 1 and 2 figure out the geometrical dimensions and the results of each calculation method of 24 examples respectively, and Fig. 6 shows the error analysis of each method.

Table 1 Geometrical dimensions of all examples

| Example No. | $h_w$/mm | $b_f$/mm | $b_t$/mm | $t_w$/mm | $t_f$/mm | $t_t$/mm | $l$/mm |
|---|---|---|---|---|---|---|---|
| 1 | | | | | | | 4,000 |
| 2 | 400 | 500 | 120 | 9 | 9 | 9 | 8,000 |
| 3 | | | | | | | 12,000 |
| 4 | | | | | | | 4,000 |
| 5 | 300 | 500 | 120 | 8 | 8 | 8 | 8,000 |
| 6 | | | | | | | 12,000 |
| 7 | | | | | | | 4,000 |
| 8 | 400 | 600 | 100 | 10 | 10 | 10 | 8,000 |
| 9 | | | | | | | 12,000 |
| 10 | | | | | | | 4,000 |
| 11 | 400 | 600 | 100 | 9 | 9 | 9 | 8,000 |
| 12 | | | | | | | 12,000 |
| 13 | | | | | | | 4,000 |
| 14 | 300 | 600 | 100 | 10 | 10 | 10 | 8,000 |
| 15 | | | | | | | 12,000 |
| 16 | | | | | | | 4,000 |
| 17 | 400 | 600 | 120 | 10 | 10 | 10 | 8,000 |
| 18 | | | | | | | 12,000 |
| 19 | | | | | | | 4,000 |
| 20 | 400 | 600 | 100 | 8 | 8 | 8 | 8,000 |
| 21 | | | | | | | 12,000 |
| 22 | | | | | | | 4,000 |
| 23 | 400 | 500 | 120 | 8 | 8 | 8 | 8,000 |
| 24 | | | | | | | 12,000 |

Table 2 Critical buckling moment, critical buckling stress and buckling modes of all examples

| Example No. | Buckling modes | Critical buckling stress /MPa | | | Critical buckling moment /kN.m | | |
|---|---|---|---|---|---|---|---|
| | | ANSYS | Eq. (68) | Jiang | ANSYS | Eq. (69) | Jiang |
| 1 | | 321.20 | 320.24 | 471.46 | 675.71 | 673.69 | 991.81 |
| 2 | Distortional | 322.00 | 319.99 | 471.46 | 677.38 | 673.15 | 991.81 |
| 3 | | 322.46 | 319.84 | 471.41 | 678.36 | 672.85 | 991.70 |
| 4 | | 259.69 | 256.27 | 373.06 | 347.85 | 343.26 | 499.70 |
| 5 | Distortional | 259.86 | 256.27 | 373.06 | 348.07 | 343.26 | 499.70 |
| 6 | | 260.22 | 256.21 | 373.02 | 348.56 | 343.18 | 499.65 |
| 7 | | 279.19 | 277.69 | 409.72 | 726.05 | 722.14 | 1,065.5 |
| 8 | Distortional | 279.61 | 277.69 | 408.72 | 727.14 | 722.14 | 1,062.9 |
| 9 | | 279.93 | 277.69 | 408.76 | 727.97 | 722.14 | 1,063.0 |
| 10 | | 226.39 | 225.12 | 331.90 | 529.41 | 526.44 | 776.12 |
| 11 | Distortional | 226.73 | 225.12 | 331.08 | 530.20 | 526.44 | 774.22 |
| 12 | | 226.98 | 225.12 | 331.12 | 530.78 | 526.44 | 774.31 |
| 13 | | 285.33 | 284.39 | 414.26 | 537.51 | 535.75 | 780.4 |
| 14 | Distortional | 285.86 | 283.50 | 413.89 | 538.52 | 534.07 | 779.7 |
| 15 | | 286.21 | 283.52 | 413.73 | 539.17 | 534.11 | 779.4 |
| 16 | | 279.16 | 276.86 | 407.00 | 742.21 | 736.10 | 1,082.1 |
| 17 | Distortional | 279.58 | 276.86 | 406.03 | 743.33 | 736.10 | 1,079.5 |
| 18 | | 279.90 | 276.86 | 406.06 | 744.17 | 736.10 | 1,079.6 |
| 19 | | 179.08 | 178.04 | 262.26 | 371.90 | 369.74 | 544.65 |
| 20 | Distortional | 179.30 | 178.04 | 261.62 | 372.37 | 369.74 | 543.32 |
| 21 | | 179.51 | 178.04 | 261.65 | 372.80 | 369.74 | 543.38 |
| 22 | | 254.16 | 253.28 | 372.56 | 474.80 | 473.15 | 695.97 |
| 23 | Distortional | 254.77 | 253.08 | 372.56 | 475.93 | 472.78 | 695.97 |
| 24 | | 255.12 | 252.97 | 372.52 | 476.59 | 472.56 | 695.90 |

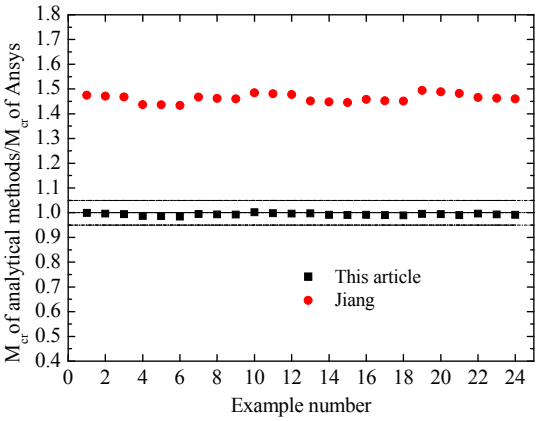


Fig. 6 Precision analysis of simplified methods

On the basis of the results, as these have been presented in Table 2 and Fig. 6, the following conclusions can be inferred:

(1) The results yielded by the calculation method, which has been introduced in this article, match well with the results of ANSYS. The limited discrepancies within the range of 3% validate the accuracy of the method, as it has been proposed in this article.
(2) The length rarely affects the critical distortional buckling moment, with the same cross-section, of a SCCBB under a negative uniform moment.
(3) The results yielded by the energy calculation method are larger than that of the finite element method under a negative uniform moment. This is owing to the restraint stiffness of the theoretical model, which is higher than that of the actual model.

## 5. Conclusions

This article revisits the traditional elastic foundation beam method and improves it by taking into account the coupling effect between the applied forces and the restraint stiffness of the bottom plate. By using a modified algorithm, this article develops a simplified calculation method for a critical distortional buckling moment of a SCCBB. This article further compares the proposed method with the traditional energy method by using the 24 examples and deduced the following conclusions:

(1) A linear coupling relationship between the applied forces and restraint stiffness of the bottom plate exists. Therefore, it may not be appropriate to use the restraint stiffness as a constant relating to the feature of a cross-section of SCCBB.
(2) The results yielded by the calculation method, as it has been introduced in this article, agree well with the finite element calculation method under a negative uniform moment. The discrepancies between the two methods are limited within the range of 3%, which validate the applicability of the method, as it has been introduced in this article.
(3) The length rarely affects the critical distortional buckling moment with the same cross-section of a SCCBB under a negative uniform moment.
(4) The results yielded by energy calculation method are larger than that of the finite element method under a negative uniform moment. Therefore, the traditional energy method is highly uncertain and needs to be improved.

## Acknowledgments

The research described in this paper was financially supported by the National Natural Science Function of China (51408449, 51378502) and the Fundamental Research Funds for the Central Universities of China (2014-IV-049).

## References

Atanackovic, T.M. and Guran, A. (2012), *Theory of Elasticity for Scientists and Engineers*, Springer-Verlag New York Inc., New York, NY, USA.

Bradford, M.A. (1988), "Buckling of elastically restrained beams with web distortions", *Thin-Wall. Struct.*, **6**(4), 287-304.

Bradford, M.A. and Gao, Z. (1992), "Distortional buckling solutions for continuous composite beams", *J.*

*Struct*. *Eng*., **118**(1), 73-89.
Bradford, M.A. and Kemp, A.R. (2000), "Buckling in continuous composite beams", *Prog*. *Struct*. *Eng*. *Mater*., **2**(2), 169-178.
British Standards Institution (1982), Code of Practice for Design of Steel Bridge, BS5400: Part 3, London, UK.
Champenoy, D., Corfdir, A. and Corfdir, P. (2014), "Calculating the critical buckling force in compressed bottom flanges of steel-concrete composite bridges", *Eur*. *J*. *Environ*. *Civ*. *Eng*., **18**(3), 271-292.
Chen, S. (1992), "Instability of composite beams in hogging bending", University of Warwick, Coventry, UK.
Chen, S. (2005), ""Experimental study of prestressed steel–concrete composite beams with external tendons for negative moments", *J*. *Construct*. *Steel Res*., **61**(12), 1613-1630.
Chen, S. and Jia, Y. (2010), "Numerical investigation of inelastic buckling of steel–concrete composite beams prestressed with external tendons", *Thin-Wall*. *Struct*., **48**(3), 233-242.
Chen, W. and Ye, J. (2010), "Elastic lateral and restrained distortional buckling of doubly symmetric I-beams", *Int*. *J*. *Struct*. *Stab*. *Dy*., **10**(05), 983-1016.
Gara, F., Ranzi, G. and Leoni, G. (2011), "Simplified method of analysis accounting for shear-lag effects in composite bridge decks", *J*. *Construct*. *Steel Res*., **67**(10), 1684-1697.
Goltermann, P. and Svensson, S. (1988), "Lateral distortional buckling: Predicting elastic critical stress", *J*. *Struct*. *Eng*., **114**(7), 1606-1625.
Ipe, T.V., Bai, H.S., Vani, K.M. and Iqbal, M.M.Z. (2013), "Flexural behavior of cold-formed steel concrete composite beams", *Steel Compos*. *Struct*., *Int*. *J*., **14**(2), 105-120.
Jaberzadeh, E., Azhari, M. and Boroomand, B. (2013), "Thermal buckling of functionally graded skew and trapezoidal plates with different boundary conditions using the element-free Galerkin method", *Eur*. *Mech*. *- A/Solids*., **42**, 18-26.
Jia, Y. and Chen, S. (2009), "Buckling coefficient of steel-concrete composite beams in negative bending", *Eng*. *Mech*., **26**(11), 121-126.
Jiang, L., Qi, J., Scanlon, A. and Sun, L. (2013), "Distortional and local buckling of steel-concrete composite box-beam", *Steel Compos*. *Struct*., *Int*. *J*., **14**(3), 243-265.
Johnson, P.R. and Fan, C.K.R. (1991), "Distortional lateral buckling of continuous composite beams", *Proceedings of the ICE-Structures and Buildings*, **91**(1), 131-161.
Lawson, M.R. and Rackham, W.J. (1989), *Design of Haunched Composit e Beams in Buildings*, Steel Construction Institution, Ascot.
Li, J., Huo, Q., Li, X., Kong, X. and Wu, W. (2014), "Dynamic stiffness analysis of steel-concrete composite beams", *Steel Compos*. *Struct*., *Int*. *J*., **16**(6), 577-593.
Liu, C., Ke, L.L., Wang, Y.S., Yang, J. and Kitipornchai, S. (2014), "Buckling and post-buckling of size-dependent piezoelectric Timoshenko nanobeams subject to thermo-electro-mechanical loadings", *Int*. *J*. *Struct*. *Stab*. *Dy*., **14**(03), 1350067.
Ruocco, E. and Minutolo, V. (2014), "Buckling analysis of mindlin plates under the green-lagrange strain hypothesis", *Int*. *J*. *Struct*. *Stab*. *Dy*., **15**(06), 1450079.
Svensson, S.E. (1985), "Lateral buckling of beams analysed as elastically supported columns subject to a varying axial force", *J*. *Construct*. *Steel Res*., **5**(3), 179-193.
Swedish Institute of Steel Construction (1982), Swedish Code for Light-Aauge Metal Structures, Stockholm, Sweden.
Timoshenko, S. (2009), *Theory of Elastic Stability*, Dover Publications Inc, New York, NY, USA.
Tinh, Q.B. and Minh, N.N. (2013), "Meshfree Galerkin Kriging model for bending and buckling analysis of simply supported laminated composite plates", *Int*. *J*. *Comp*. *Meth*.*-Sing*., **10**(03), 1350011.
Tong, G. and Xia, J. (2007), "Buckling of I-sectional steel beams loaded by negative moments", *Prog*. *Steel Build*. *Struct*., **9**(1), 46-51.
Wang, D. and Peng, H. (2013), "A Hermite reproducing kernel Galerkin meshfree approach for buckling analysis of thin plates", *Comput*. *Mech*., **51**(6), 1013-1029.
Williams, F.W. and Jemah, A.K. (1987), "Buckling curves for elastically supported columns with varying

axial force, to predict lateral buckling of beams", *J. Constuct. Steel Res.*, **7**(2), 133-147.
Ye, J. and Chen, W. (2013), "Elastic restrained distortional buckling of steel-concrete composite beams based on elastically supported column method", *Int. J. Struct. Stab. Dy.*, **13**(1), 1-29.
Zhou, W., Jiang, L. and Yu, Z. (2012), "The distortional buckling calculation formula of the steel-concrete composite beams in the negative moment region", *Chinese J. Computat. Mech.*, **29**(3), 446-450.
Zhou, W., Jiang, L., Kang, J. and Bao, M. (2014), "Distortional buckling analysis of steel-concrete composite girders in negative moment area", *Math. Probl. Eng.*, **2014**(1), 1-10.
Zhou, W., Li, S., Jiang, L. and Qin, S. (2015), "Vibration analysis of steel-concrete composite box beams considering shear lag and slip", *Math. Probl. Eng.*, **2015**(1), 1-8.

*CC*